The effect of doping and processing conditions on the optical performance of Rh:$BaTiO_3$

Małgosia Kaczmarek[1], Robert W. Eason[2], Irina Mnushkina[3]

[1] School of Physics, University of Exeter, Exeter EX4 4QL, United Kingdom,
fax: +44 1392 264111, e-mail: M.Kaczmarek@exeter.ac.uk.

[2] Optoelectronics Research Centre and Department of Physics and Astronomy, University of Southampton, Southampton SO17 1BJ, United Kingdom

[3] Deltronic Crystal Industries Inc, 60 Harding Avenue, Dover, New Jersey 07801, United States

Abstract

We demonstrate the advantages of using high levels of rhodium (2000-3200 ppm) to dope barium titanate for achieving finite absorption coefficients (0.36 cm^{-1}), high two-beam coupling gain (11.5 cm^{-1}) and acceptable response time (7 s) at 1.06 μm. We also report on the mass spectroscopy measurements on Rh:$BaTiO_3$ samples indicating a small segregation coefficient for rhodium (below 0.01) and the presence of a relatively large concentration (6000 ppm) of unintentionally added strontium.

PACS: 42.25.Bs, 42.70.Nq, 85.40.Ry.

1. Background

Since the first results on 'blue', rhodium doped $BaTiO_3$ were published five years ago[1,2], there has been a lot of interest in this new type of photorefractive material. Its attractive features, such as high self-pumped phase conjugate reflectivities[1] and record high two-beam coupling gains[3] achieved both in the visible and the infrared, stimulated a lot of research into exploring its potential and characterising its properties[4]. The infrared sensitivity of Rh:$BaTiO_3$ has been of particular interest, and several significant results have been published recently on its response to 1.06 μm radiation. Very high two-beam coupling gain[5] (23 cm^{-1}) was measured in a specially cut sample, and 9.1 cm^{-1} in an uncut sample[6] of Rh:$BaTiO_3$ using cw 1.06 μm light. Considerable phase conjugate reflectivities, as high as 50-55% have been observed[6,7]. Similar promising results have been obtained with nanosecond 1.06 μm pulses[8,9]. As a result, efficient beam clean-up of an Nd:YAG beam has been observed[10,11] and an efficient ring self-pumped phase conjugate mirror optimised[12]. In parallel with these experimental investigations, theoretical modelling was

carried out to characterise the valence states of impurities present. It has been shown that both Rh^{3+}/Rh^{4+}, as well as Rh^{4+}/Rh^{5+} ions are responsible for photorefractive behaviour[13,14]. A three valence state system[15,16] has therefore been used to model the experimental results and to characterise the photorefractive parameters[17,18,19] of Rh:$BaTiO_3$.

In spite of this considerable progress in characterising, both experimentally and theoretically, the optical properties of Rh:$BaTiO_3$, the question of the optimum amount of doping and growth/ processing conditions for the most efficient response above 1 μm has still remained largely unresolved. We have addressed this issue in our work. The aim of our research was also to identify all the impurities that give this material much better photorefractive performance in the infrared region than nominally undoped $BaTiO_3$.

2. Introduction

We have investigated several samples of Rh:$BaTiO_3$ doped with different amounts of rhodium and processed under different conditions. Table 1 lists the samples we investigated, detailing the amount of rhodium added to the melt, and post-growth processing conditions. The most comprehensive comparison we were able to make involved samples with 400 ppm of rhodium added to the melt[20]: samples 1-3 came from the same boule, but sample 4 was grown and processed separately, but under the same conditions. Sample 10 was the original, 'blue' Rh:$BaTiO_3$ that was accidentally doped with rhodium during growth[1].

The growth and processing conditions determine the relative concentrations of the respective valence states of rhodium (Rh^{3+}, Rh^{4+} and Rh^{5+}), other impurities such as iron, and oxygen vacancies. In the case of our samples, after growth the boule was slowly cooled down to room temperature at the rate of 25°C per hour. The crystals were then cut from the boule, and the as-grown sample was left unprocessed. The samples annealed in oxygen were purposely annealed under an oxygen flow atmosphere at normal pressure, with a flow rate of 0.5 l/min. The annealing was done at the temperature of 1000°C for 24 hours. The samples were then quenched to fix the oxygen concentration. They were cooled down fast, from 1000°C to 300°C, within one hour and then slowly cooled down through the phase transition (25°C/hour) to the room temperature. The annealed in air samples were annealed at the same conditions, but with air atmosphere instead of oxygen flow. Annealing in air at 1000°C corresponds to creating an environment around the crystal that had relatively low concentration of oxygen, i.e. lower than in the two previous cases, and can be regarded as a reducing environment.

3. Mass spectroscopy

Since the first blue Rh:$BaTiO_3$ crystals were grown, one of the most interesting questions was to identify all the impurities present. This problem was particularly important, as the amount of rhodium, and other impurities, added to the melt was unknown. Since these original, blue crystals showed exceptional photorefractive performance[1,3], the information about the type and amount of dopants was essential for growing new, infrared sensitive and highly efficient samples. The other critical issue concerned the final concentration of rhodium in the crystal, compared to that in the melt.

Mass spectroscopy was performed using a VG Elemental ICP-MS coupled to a Spectron Systems UV laser. The analyses were carried out at various sites over the surface of the crystals. At each site the laser was fired for a period of 30 seconds producing a 20 μm diameter pit. Data was acquired for ^{103}Rh and ^{107}Ag in peak jumping mode. In the absence of a suitable Rh standard, Ag data was acquired from a NIST 610 glass standard to derive an approximate calibration factor. Ag was chosen because of its proximity to Rh in atomic mass, and because of its certified concentration in the standard.

Table 2 summarises the results obtained from mass spectroscopy performed on the original, blue Rh:$BaTiO_3$ and on the 400 ppm intentionally doped Rh:$BaTiO_3$. These data are compared with typical results[2] from a nominally undoped $BaTiO_3$.

The results show that, firstly, approximately between 2- 4 ppm of rhodium were actually detected in the 400 ppm sample. The average concentration detected was 2.6±0.2 ppm. The ratio of the amount of rhodium found in the crystals to the amount added to the melt can then be calculated to give the magnitude of segregation coefficient. In our case it was very small, between 0.005 to 0.01, with the average value of 0.007 and a standard error of 5×10^{-4}. If the upper and lower limit of this coefficient is also assumed for the original Rh:$BaTiO_3$, the 14 ppm of rhodium detected in the crystal implies a rhodium concentration of 1400-2800 ppm in the melt. The concentration of rhodium in both samples is surprisingly low, considering the dramatic improvement in photorefractive performance of Rh:$BaTiO_3$, compared with nominally undoped $BaTiO_3$.

The level of strontium, which wasn't purposely added to the melt, was in contrast surprisingly high. While it is usually present in nominally undoped $BaTiO_3$ at typical concentrations of around 2000 ppm, the original sample has three times and the 400 ppm sample approximately

1.5 times this value. Strontium substitutes for barium, generally changing the width of the bandgap and lowering the Curie temperature[21].

The only other significant impurity found was cobalt, but at relatively low concentrations (less than 10 ppm). Other elements, such as Mg, Al, Ca, Cr, Mn, Fe, Ni were also detected, but at concentrations comparable with the detection limit. The detection limit for these elements was relatively high, namely 10 ppm, caused by instrument interferences and existing contamination.

These results confirm that rhodium is indeed the most significant impurity and no other transition metal is present in detectable amounts. However, the exact role of strontium and its relatively large concentration, is still not clear yet.

4. Absorption coefficient measurements

Absorption spectra of all the samples examined, except one, show similar features, namely a characteristic[1], pronounced increase of absorption around 650 nm and finite absorption around 800 nm with a broadened absorption 'tail' extending to above 1 μm. The only exception was the annealed in air sample (400 ppm). Figure 1 shows the absorption spectra of this sample (Sample 3) together with spectra of the 400 ppm as-grown (Sample 1) and annealed in oxygen (Sample 2) crystals. Since all of these samples came from the same boule, this comparison illustrates how annealing in air lowered the absorption coefficients across the spectrum. For comparison, at 650 nm the absorption coefficient was only 0.34 cm^{-1}.

The explanation for the differences between these three absorption spectra can be suggested using the three valence state model[13,15]. The increase of absorption around 650 nm is usually attributed to Rh^{4+}, and around 800 nm to Rh^{5+}. The spectrum of as-grown sample (Sample 1) shows the characteristic peak at 650 nm, indicating the presence of Rh^{4+}. An oxidising atmosphere applied to Sample 3 (annealed in oxygen) would contribute to the conversion of Rh^{4+} into Rh^{5+}. Indeed, some increase of absorption around 800 nm observed in this sample would confirm the presence of such process. However, no decrease of absorption around 650 nm was measured. It is suggested that either only a small proportion of Rh^{4+} transformed to Rh^{5+} or that the balance of Rh^{4+} concentration was restored by the transfer of Rh^{3+} to Rh^{4+}. Finally, the reducing atmosphere created during the annealing in air of Sample 2 would contribute to the conversion of Rh^{4+} into Rh^{3+}. It is therefore expected that the absorption would decrease around 650 nm. The significant decrease of absorption, across the visible and near-infrared spectrum,

observed in this sample would suggest that it was significantly reduced during annealing, making Rh^{3+} the dominant valence state.

In contrast, the other 400 ppm annealed in air sample (Sample 4) had a relatively high absorption, measured as 4.12 cm^{-1} at 650 nm. It transpires that in spite of careful control of growth and processing conditions, the samples doped with little rhodium could have quite different absorption coefficients, and hence very different optical response. Similar problems have been encountered when growing nominally undoped $BaTiO_3$.

A comparison was then made of absorption spectra from three 3200 ppm samples[23] (Samples 6, 7 and 8), as presented in Figure 2. These three samples came from different boules and one of them was annealed in oxygen after growth. Despite this, their spectra were almost identical. One conclusion is that adding more rhodium can prevent other accidental impurities being incorporated in the crystal, thereby ensuring a better control of absorption in different samples of heavily doped Rh:$BaTiO_3$.

In general, the absorption spectra of the 2400, 3200 and 5000 ppm samples were very similar. They all have finite value of absorption at 1.06 μm, that ranged in the 2400 and 3200 ppm samples from 0.2 to 0.36 cm^{-1}, and 0.11 cm^{-1} in the 5000 ppm sample. This result would suggest that the optimum amount of rhodium, for high absorption in the near-infrared, lies within the 2400-3200 ppm range. This coincides with the inferred approximate range of 1400-2800 ppm of rhodium (added to the melt), suggested by mass spectroscopy for the original, blue Rh:$BaTiO_3$ sample.

Two of the samples we investigated, the 2400 ppm and the 'new' 3200 ppm also have measurable absorption at 1.3 μm, equal to 0.15 and 0.08 cm^{-1}, respectively. These coefficients indicate the possibility of observing two-beam coupling gain at this important telecommunications wavelength.

5. Two-beam coupling at 1.06 μm

We tested the ten samples of Rh:$BaTiO_3$ for the magnitude of two-beam coupling (TBC) gain at a common grating spacing of 1.49 μm, using a cw single-longitudinal mode miniature Nd:YAG laser for signal and pump beams. Both beams were linearly polarised. We defined the gain as the ratio of the signal beam intensity with and without the pump beam present[3]. The first sample we considered was the annealed in air 400 ppm sample (Sample 3) that had the unusually low absorption. Since this sample did not show any gain at 1.06 μm, we tested it at 514.5 nm. The gain we measured was very small, yielding a coupling coefficient Γ equal to 2.4 cm^{-1} (as

compared with 14.9 cm^{-1} measured in the 400 ppm as-grown sample). In order to eliminate the possibility of this crystal being depoled, we poled it again, and then measured TBC gain for the second time. The coupling coefficient we measured was only slightly higher than in the first case, namely 2.45 cm^{-1}. We could therefore suggest that annealing in air brought this sample close to the compensation point, where the contributions from electron and hole transport cancel each other, yielding a negligible net photorefractive effect[22]. The work on more detailed, theoretical explanation and modelling of this effect is currently under way.

Our studies of TBC optical performance of the rest of the samples are summarised in Table 3 and compared with other published results. The coupling coefficients we measured at 1.06 μm were quite high with values of 8.7 cm^{-1} and 11.2cm^{-1}, even in samples where absorption was negligible (0.03 and 0.06 cm^{-1}). The gain also appears not to be directly proportional to the amount of rhodium added. Nevertheless, the highest coupling coefficients, from 8.5 to 11.5 cm^{-1}, were measured in heavily doped samples, with 3200 ppm of rhodium added to the melt. Adding even more rhodium does not seem to improve the optical performance, as in the 5000 ppm sample, a coupling coefficient of only 6 cm^{-1} was measured.

This analysis, although largely qualitative nevertheless provides important information, particularly useful for choosing the best Rh:$BaTiO_3$ sample for applications requiring, for example high gain with low absorption coefficients[23].

6. Response time measurement

Although the value of TBC gain is not directly proportional to the value of absorption coefficient, the response time clearly depends on absorption. The build-up of a grating in crystals with negligible absorption (approximately below 0.1 cm^{-1}) takes some minutes, which may pose a problem in most applications. On the other hand, the samples with absorption above 0.1 cm^{-1}, namely samples 1-9, showed acceptable and more usable response times. Figure 3 presents data on response time, τ, defined as the 10% to 90% rise time of the TBC gain steady-state value. The smallest value of τ we recorded was 7 seconds at 4W/cm^2. Because of the limited laser power we could not check the response time at higher intensities, but the extrapolation of the experimental data suggests that at 14 W/cm^2, we could expect response time to reach 2 s. This is consistent with the result published by Brignon *et al.*[6] where the response time of 4 s was measured at 14 W/cm^2. On the other hand, the record high TBC gain reported by Huot *et al.*[5] seems to take much longer time to develop, namely 75 s at 18.8 W/cm^2. However, the dependence between intensity and response time reported there, i.e. τ being simply inversely

proportional to intensity, also applies in the case of our Rh:$BaTiO_3$ samples. The solid lines in Figure 3 show that this straightforward dependence, namely $\tau \propto I^{-x}$, where x=1, is in fact the best fit to the experimental results in all our samples.

6. Conclusions

We have investigated several samples of Rh:$BaTiO_3$ doped with different amount of rhodium and processed in different conditions to determine the best growth and material parameters for efficient response in the infrared.

Mass spectroscopy revealed that very little rhodium, out of the amount added to the melt, ends up in the crystal. One may speculate that because of such a small segregation coefficient other accidental impurities may also get incorporated instead, if little rhodium is added. Moreover, the samples with only 400 ppm of rhodium added to the melt were more sensitive to changes in growth and processing conditions than the samples with 3200 ppm of rhodium added to the melt.

We have demonstrated that the TBC gain at 1.06 μm was the highest in the heavily doped crystals (3200 ppm) and relatively high absorption coefficients meant the promising speed of building up of this gain, i.e. as fast as 7 seconds at 4 W/cm^2. Considering the values of absorption, TBC gain and the response time, the optimum doping with rhodium is approximately 2000-3200 ppm added to the melt. We have shown that adding more rhodium than this range does not improve the photorefractive performance of Rh:$BaTiO_3$.

The analysis of doping and growth conditions presented here is a basis for developing a model to calculate systematically the photorefractive parameters of these crystals. The work on this model is currently under way and aims to provide a better insight into the type and the number of centres involved in photorefractive effects in Rh:$BaTiO_3$.

7. Acknowledgements

We would like to thank Mark Garrett of Nonlinear Photonics for supplying us with Rh:$BaTiO_3$ and for useful advice and collaboration on this work. We would also like to thank Mike Damzen and Laura Corner for valuable advice and discussions, Gerald Roosen for his constructive comments and Arnaud Brignon for interesting discussions. We thank Andy Milton for his assistance in mass spectroscopy measurements.

We gratefully acknowledge the financial support of the Royal Society Research Grant Scheme and the Engineering and Physical Sciences Research Council (EPSRC) under grant number GR/M/11844.

8. References

[1] G. W. Ross, P. Hribek, R.W. Eason, M. H. Garret and D. Rytz, Opt. Commun. **101**, (1993) 60.

[2] C. Warde, T.S. McNamara. M.H. Garrett and P. Tayebati, SPIE Conference, San Diego CA, (1993) CR48-07.

[3] M. Kaczmarek. R. W. Eason, Optics Lett. **20**, 1850 (1995).

[4] B. A. Wechsler, M. B. Klein, C. C. Nelson, R. N. Schwartz: Opt. Lett. 19, 536 (1994).

[5] N. Huot, J. M. C. Jonathan, G. Pauliat, D. Rytz, G. Roosen: Opt. Comm. **135**, 133 (1997).

[6] A. Brignon, D. Geffroy, J. P. Huignard, M. H. Garrett, I. Mnushkina: Opt. Comm. **137**, 311 (1997).

[7] N. Huot, J. M. C. Jonathan, D. Rytz, G. Roosen: Opt. Comm. **140**, 296 (1997).

[8] A. Brignon, J. P. Huignard, M. H. Garrett, I. Mnushkina: Opt. Lett. **22**, 215 (1997).

[9] N. Huot, J. M. C. Jonathan, G. Roosen, D. Rytz: Opt. Lett. **22**, 976 (1997).

[10] A. Brignon, J. P. Huignard, M. H. Garrett, I. Mnushkina: Appl. Opt. **36**, 7788 (1997).

[11] A. Brignon S. Senac, J. L. Ayral, J. P. Huignard: Appl. Opt. **37**, 3990 (1997).

[12] N. Huot, J. M. C. Jonathan, G. Roosen: J. Opt. Soc. Am. B **15**, 1992 (1998).

[13] H. Kröse, R. Scharfschwerdt, O. F. Schirmer, H. Hesse: Appl. Phys. B **61**, 1 (1995).

[14] U. van Stevendaal, K. Buse, S. Kämper, H. Hesse. E. Krätzig: App. Phys. B **63**, 315 (1996).

[15] K. Buse, E. Krätzig: App. Phys. B **61**, 27 (1995).

[16] K. Buse, S. Loheide, D. Sabbert, E. Krätzig: J. Opt. Soc. Am. B **13**, 2644 (1996).

[17] N. Huot, J. M. C. Jonathan, G. Roosen: Appl. Phys B **65**, 489 (1997).

[18] L. Corner, R. Ramos-Garcia, A. Petris, M. J. Damzen: Opt. Comm. **143**, 165 (1997).

[19] L. Corner, M. J. Damzen: Proc. CLEO/Europe, Glasgow, 1998, CThH57, 298 (1998).

[20] M. Kaczmarek, R.W. Eason, G. Maatz, M.H. Garrett, I. Mnushkina: Proc. 1997 Topical Meeting on Photorefractive Materials, Effects and Devices, TP10, Chiba, Japan, (1997).

[21] M. H. Garrett: *private communication*

[22] B. A. Wechsler, M. B. Klein, D. Rytz: SPIE vol.681, Laser and Nonlinear Optical Materials, 91 (1986).

[23] M. Kaczmarek, R. W. Eason: Opt. Comm. **154**, 334 (1998).

Figure captions

Figure 1 Absorption spectra of Rh:BaTiO3 samples with 400 ppm added to the melt. Solid curve: as-grown sample; dashed curve: annealed in air sample; dash-dot curve: annealed in oxygen sample.

Figure 2 Absorption spectra of Rh:BaTiO3 samples with 3200 ppm added to the melt. Solid curve: as-grown sample, dashed curve: 'new' as-grown sample, dash-dot curve: annealed in oxygen sample.

Figure 3 Two-beam coupling response time at 1.06 mm. Symbols represent experimental data and solid lines a theoretical fit assuming $\tau \propto I^{-x}$, where x =1. For comparison, the experimental results from reference [5] are shown (as 'O') and from reference [6] (as' Δ ').

TABLE 1 Rh:$BaTiO_3$ samples

Sample	Rhodium added to the melt and processing	References
1	400 as-grown	[20]
2	400 annealed in oxygen	"
3	400 annealed in air	"
4	'new' 400 annealed in air	
5	2400 ppm as-grown	[23]
6	3200 as-grown	"
7	'new' 3200 as-grown	"
8	3200 annealed in oxygen	"
9	5000 ppm as-grown	"
10	original, 'blue' sample[1]	[1]

TABLE 2 - Mass spectroscopy of $Rh:BaTiO_3$

	original blue $Rh:BaTiO_3$	400 ppm $Rh:BaTiO_3$	standard error	nominally undoped $BaTiO_3$
rhodium added to the melt	unknown	400 ppm		N/A
rhodium in the crystal (ppm)	14	2-4	0.2	0.5
cobalt (ppm)	< 10	< 10	0.2	below 0.2
major impurity present: Sr (ppm)	> 6000	3000	1	> 2000

TABLE 3 - Infrared performance of Rh:$BaTiO_3$ crystals

	α at 1.06 μm [cm^{-1}]	Γ [cm^{-1}]	References
400 as-grown (sample 1)	0.03	8.7	our work
'new' 400 as-grown (sample 4)	0.14	6.0	"
2400 ppm (sample 5)	0.27	7.8	"
3200 as-grown (sample 6)	0.2	8.5	"
'new' 3200 as-grown (sample 7)	0.36	9.3	"
3200 annealed in O_2 (sample 8)	0.25	11.5	"
5000 ppm (sample 9)	0.11	6.0	"
Original blue (sample 10)	0.06	11.2	[3]
2000 ppm, specially cut sample	0.15	23	Huot *et al.* [5]
3200 ppm Rh:$BaTiO_3$	0.13	9.1	Brignon *et al.* [6]

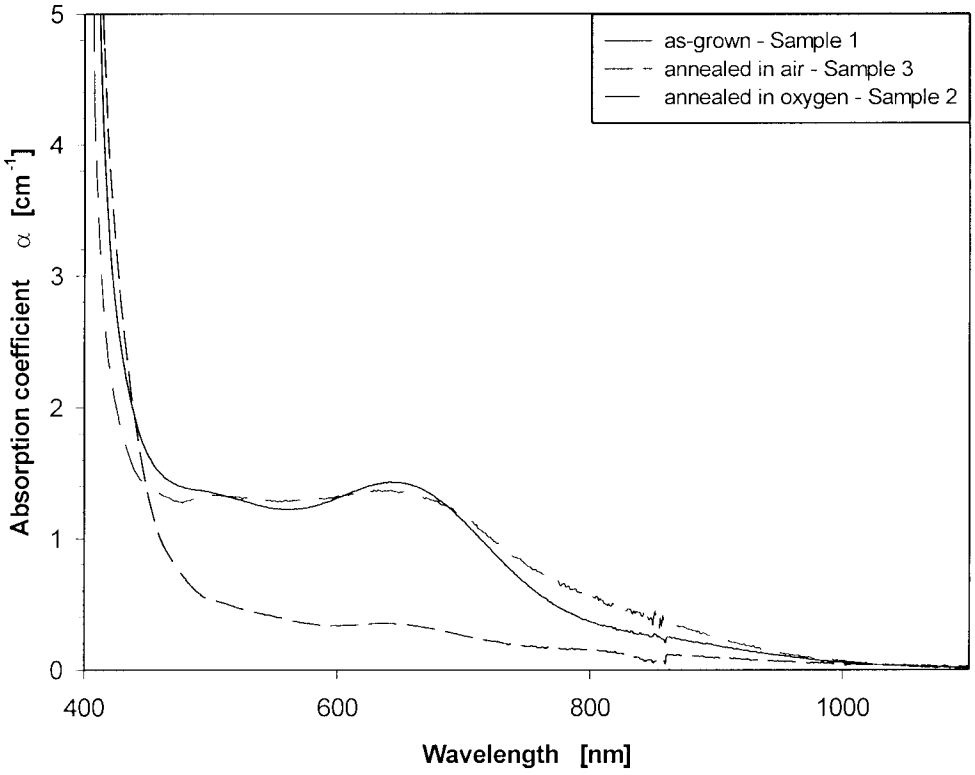
as-grown - Sample 1
annealed in air - Sample 3
annealed in oxygen - Sample 2
Absorption coefficient α [cm-1]
Wavelength [nm]
0
1
2
3
4
5
400
600
800
1000

Fig 1

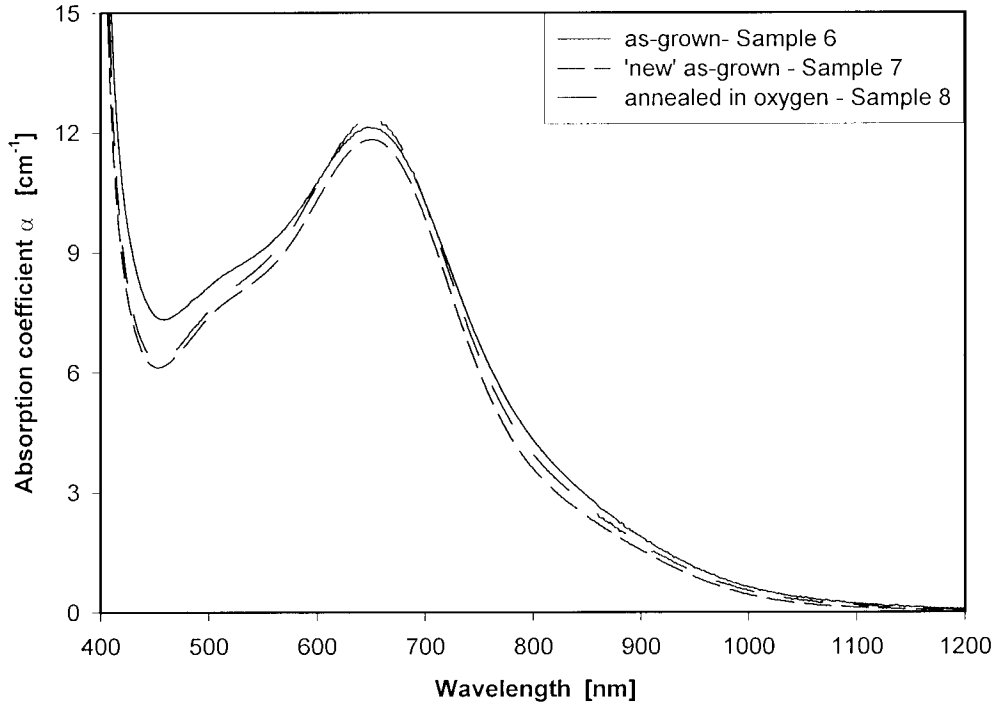
as-grown- Sample 6
'new' as-grown - Sample 7
annealed in oxygen - Sample 8
Absorption coefficient α [cm-1]
Wavelength [nm]
0
3
6
9
12
15
400
500
600
700
800
900
1000
1100
1200

Fig 2

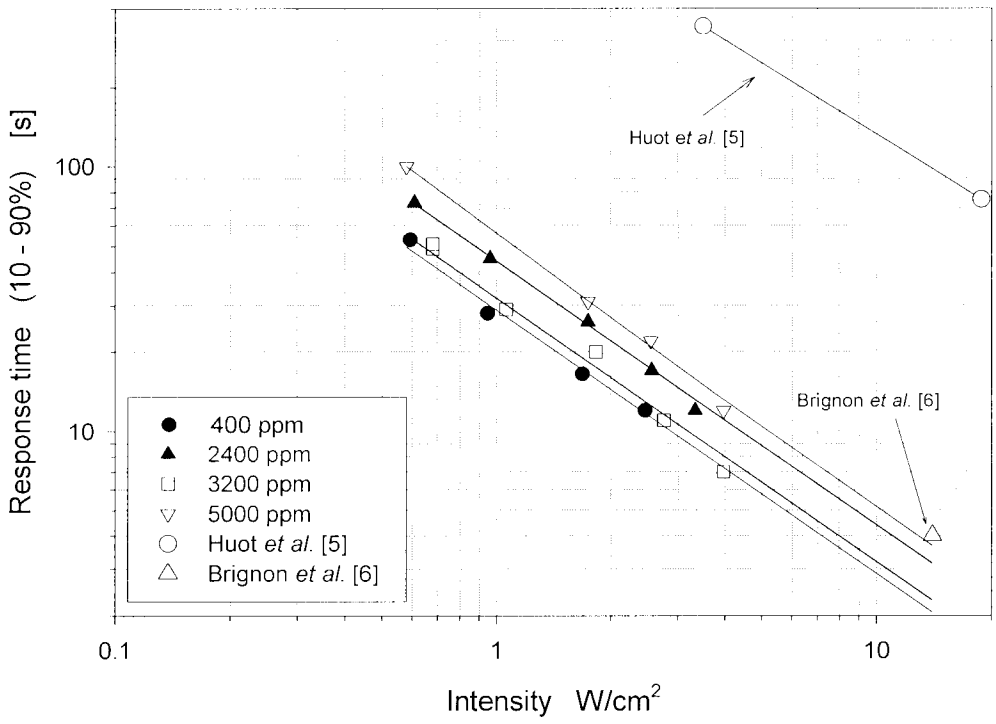
Response time (10 - 90%) [s]
100
10
0.1
1
10
Intensity W/cm^2
Huot *et al.* [5]
Brignon *et al.* [6]
400 ppm
2400 ppm
3200 ppm
5000 ppm
Huot *et al.* [5]
Brignon *et al.* [6]

Fig 3